# Spin-Polarised edge states in atomic manganese chains supported on $Cu_2N$ / Cu (100)

**Deung-Jang Choi**‡

CIC nanoGUNE, Tolosa Hiribidea 78, Donostia-San Sebastián 20018, Spain

**Roberto Robles**

Catalan Institute of Nanoscience and Nanotechnology (ICN2), CSIC
The Barcelona Institute of Science and Technology, Campus UAB, Bellaterra, 08193 Barcelona, Spain

**Jean-Pierre Gauyacq**

Institut des Sciences Moléculaires d'Orsay (ISMO), CNRS, Univ. Paris-Sud, Université Paris-Saclay, Bât. 351, 91405 Orsay CEDEX, France

**Carmen Rubio Verdú**

CIC nanoGUNE, Tolosa Hiribidea 78, Donostia-San Sebastián 20018, Spain

**Nicolás Lorente**

Centro de Física de Materiales CFM/MPC (CSIC-UPV/EHU), Paseo Manuel de Lardizabal 5, 20018 Donostia-San Sebastián, Spain
Donostia International Physics Center (DIPC), Paseo Manuel de Lardizabal 4, 20018 Donostia-San Sebastián, Spain

**José Ignacio Pascual**

CIC nanoGUNE, Tolosa Hiribidea 78, Donostia-San Sebastián 20018, Spain
Ikerbasque Basque Foundation for Science, 48013 Bilbao, Spain

**Abstract.** Scanning tunnelling microscopy and density functional theory studies of manganese chains adsorbed on $Cu_2N$/Cu (100) reveal an unsuspected electronic edge state at $\sim$ 1 eV above the Fermi energy. This Tamm-like state is strongly localised to the last Mn atom of the chain and fully spin polarised. However, no equivalence is found for occupied states, and the electronic structure at $\sim -1$ eV is mainly spin unpolarised due to the extended $p$-states of the N atoms that mediate the coupling between the Mn atoms in the chain. The spin polarisation of the edge state is affected by the antiferromagnetic ordering of the chains leading to non-trivial consequences.

‡ Corresponding author: d.choi@nanogune.eu

## 1. Introduction

Magnetic nanochains are experiencing a lot of interest due to their quasi 1-D character that confers them with extraordinary properties [1]. Atomic magnetic nanochains are the best examples of what magnetic nanodevices can achieve and how they can be instrumental for spintronics [2]. These chains are assembled using the atom manipulation capabilities of the scanning tunnelling microscope (STM). Magnetic atoms have been positioned one by one at different distances and with different arrangements on a variety of substrates [3, 4, 5, 6, 7, 8]. The STM has permitted to characterise the chains by their spin signature using spin-polarised tips [9] and by their inelastic electron tunnelling spectra (IETS) [10, 11]. These measurements give unprecedented insight into the atomic mechanisms leading to magnetic ordering in nanostructures that can be compared with state-of-the-art theoretical results.

Theoretical works are generally based on density functional theory (DFT) studies. These works evaluate the actual atomic arrangements of the atoms on the surface, the local and global magnetic moments, as well as the magnetic anisotropy energies, the exchange couplings among the chain constituents and the possibility of canting due to the Dzyaloshinskii-Moriya interaction. For the case of Mn chains on Ni (100), Lounis and co-workers [12] showed that the competition of the different exchange couplings in the system led to an even/odd effect with the number of Mn atoms; even-numbered chains presenting a non-collinear arrangement of their spins and chains with an odd number of atoms a collinear antiferromagnetic ordering. Rudenko and collaborators [13] performed thorough calculations of Mn chains on a $Cu_2N$/Cu (100) substrate. They reproduced the exchange couplings between atoms that lead to magnetic excitation spectra in good agreement with the experimental ones [3]. Another complete study of Mn and Co chains on $Cu_2N$/Cu (100) was performed by Lin and Jones [14] where they extended their previous results [15] and confirmed that the atoms maintain their nominal spins on the surface, $S$=5/2 for Mn. Nicklas and co-workers [16] studied Fe chains on $Cu_2N$/Cu (100) showing that as for Mn, [13] N-mediated superexchange leads to antiferromagnetic coupling of the Fe atoms, in good agreement with later experimental measurements [5]. The interpretation of these experiments has shown the importance of correlation and entanglement in these antiferromagnetic chains [17]. Urdaniz *et al.* [18] performed a thorough study of Cr, Fe, Mn and Co chains on $Cu_2N$/Cu (100) using DFT calculations showing that the adsorption site determines to a great extent the type of magnetic coupling of the chain as recently corroborated [19, 20]. This is presently used to generate atomic chains with different coupling schemes [21].

All these works focus in the low-energy structure tunnelling conductance spectra that has a direct link to the magnetic properties of the crafted nano-objects. Surprisingly, no work has been studied on the larger energy scale that actually has influences on the magnetic properties of these systems. In the present work, we report on the electronic structure with a special attention to states originating in orbitals more extended than pure $d$-electrons. We show that there are long-lived edge states

that maintain strict localisation. These edge states are Tamm states [22] due to the unsaturated bond of the edge Mn atom. These edge states are at $\sim 1$ eV above the Fermi level. A broader resonance is also found for occupied states at about $\sim -1$ eV. However, there are no specific magnetic features associated with this state and it is rather a state originating in the covalent bonding of the Mn atoms with the N atoms glueing the Mn chain together. The magnetic structure of the Mn chains are due to the spin polarization of the *d*-electrons, much lower in energy than the $\sim -1$ eV structure of the N-Mn bonds.

## 2. Experimental method

Experiments were performed in an ultrahigh-vacuum low-temperature STM at a base temperature of 1.15 K, using a Joule-Thomson cooling stage in a SPECS-JT STM. The differential conductance was directly measured using lock-in detection with a sample bias, V, with a modulation of 2mV rms for conductance spectra when we required higher bias resolution; we used a 10mV rms modulation for conductance maps obtained at fixed bias. Both modulations were performed at 938.6 Hz.

The Cu(100) surface was cleaned by Ar sputtering and then annealed up to 650 K. After having large terraces over the Cu(100) surface, a monolayer of $Cu_2N$ was formed as a decoupling layer by N irradiation [23, 24]. Single Mn atoms were deposited onto the cold surface directly at the STM stage. By capturing the Mn atom with the tip and dropping it onto the substrate via bias pulses, the single atoms were arranged into closed-packed Mn chains along the [010]-direction of the $Cu_2N$ surface. This leads to mono-atomic chains of Mn atoms ontop of Cu atoms that are aligned along a nitrogen row, identical to the structures reported in Ref. [3].

## 3. Theoretical method

*Ab initio* calculations were performed within the density-functional theory (DFT) framework as implemented in the VASP code [25]. We have expanded the wave functions using a plane-wave basis set with a cutoff energy of 300 eV. Core electrons were treated within the projector augmented wave method [26, 27]. The Perdew-Burke-Ernzerhof (PBE) form of the generalised gradient approximation (GGA) was used as exchange and correlation functional [28]. To model the surface, we have used a slab geometry with four Cu layers plus the $Cu_2N$ layer. We have used an optimised theoretically lattice constant for Cu of 3.65 Å.

Following the above experimental procedure, the transition-metal atoms are positioned on Cu atoms, forming a chain in the [010] direction. We have used a unit cell that increases its size along this direction with the number of atoms of the chain as $[3 \times (n{+}3)]$, where $n$ is the number of Mn atoms. In this way, we keep the distance between chain images constant for all sizes, being of 3 lattice constants in the unrelaxed configuration. The bottom Cu layer was kept fixed and the remaining atoms were

allowed to relax until forces were smaller than 0.01 eV/Å. The $k$-point sample was varied accordingly to the unit cell, and tests were performed to assure its convergence.

In order to account for the atomic magnetic moments of the Mn atoms on the surface, we have used the local Coulomb integral $U$, and the exchange integral, $J$ to correct the energy. The scheme of Dudarev *et al* [29] was employed, with a $U_{\texttt{eff}} = U - J$ of 4 eV. The chosen value corresponds to roughly substracting $J \approx 1$ from $U = 4.9$ eV as computed by Lin and Jones [14] for Mn ontop a Cu atom.

## 4. Results

### *4.1. Scanning tunneling spectroscopy of electronic states*

Constant current STM images obtained for sample biases above 1V show that the Mn chains develop a "dumbell" shape and present enhanced states at the edges. Figure 1 ($a$) shows the image obtained at $V_s = 2$ V. Here, the distortion is evident for $Mn_5$ and $Mn_6$. Mapping the conductance at a fixed sample bias of 1V gives direct evidence of the localisation of the contributing electronic states. Indeed, Fig. 1 ($b$) shows that most of the conductance is located on the borders of the corresponding protrusions of Fig. 1 ($a$). However, no edge features can be appreciated at negative bias. Figure 1 ($c$) depicts the constant current image at -1V and a featureless protrusion straddles the atoms of the chain. Consequently, the corresponding dI/dV map (not shown) does not reveal any localisation inside the chain.

In order to gain more insight, we plot in Fig. 1 ($d$) the conductance as a function of bias for three different positions over the $Mn_6$ chain. When the tip is above a chain's edge, a distinct peak is detected at 1V, which is not present on the spectrum at the centre. This is in good correspondence with Figs. 1 ($a$) and ($b$), and strongly suggests that there is an unoccupied electronic state localised at the edges of the Mn chains. For negative biases, a broader peak at $\sim -1$ V is observed with larger intensity at the centre of the chain. From these data, we conclude that an electronic edge state appears at $\sim 1$ V, while for occupied states an electronic state appears at $\sim -1$ V with a broader line shape, and extended along the chain.

Figure 2 displays the tunnelling conductance as a function of bias as well as the conductance spectra as a function of bias and position taken along the chain for $Mn_2$, $Mn_3$, $Mn_4$, and $Mn_5$. The figure displays raw data with a linear colour code with values ranging from 0 to 4 nS. The background (depicted as a black line on the upper panels) was obtained by measuring on a clean spot on the surface. It presents a gap-like behaviour due to the appearance of states confined to the upper layer of the substrate beyond $\approx$ 2 V and below $\approx$ -2 V, this energy scale nicely corresponds to the $Cu_2N$ gap [24]. The consequence is that intrinsic chain states are easier to detect in an energy window of roughly 4 eV about the Fermi energy. Two clear features appear at empty and occupied states (about $\sim \pm 1$ V) for all chains. As the size of the Mn chains is reduced, the features for occupied states evolve becoming very broadened and

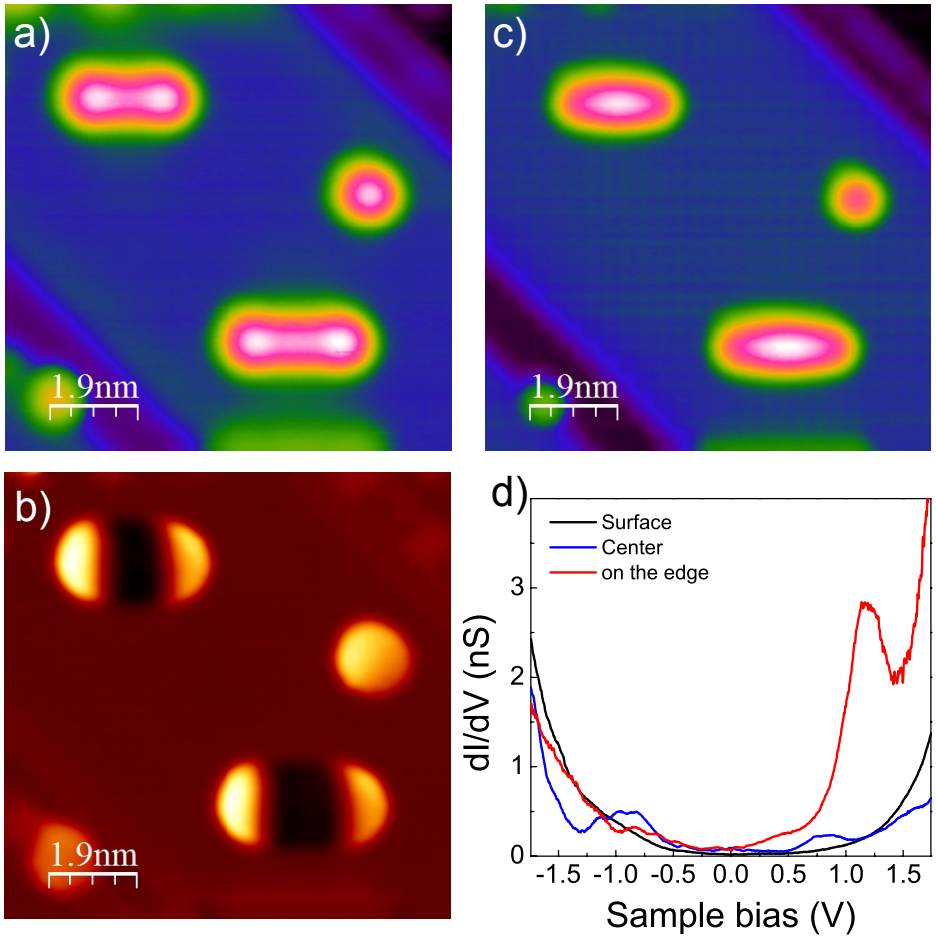


**Figure 1.** (*a*) Constant current image taken at 2 V showing a $Mn_5$ chain (upper left corner) and a $Mn_6$ chain (bottom centre) ($V_s$ = 2 V, $I_t$ = 100 pA). (*b*) Conductance map at 1 V over the same area ($V_s$ = 1 V, $I_t$ = 1 nA). The prevailance of the edges of the chains is clearly seen as maxima in the conductance. (*c*) The constant current image at -1 V is rather featureless over all the chains ($V_s$ = -1 V, $I_t$ = 100 pA). (*d*) The tunnelling conductance as a function of applied bias over two different spots on the $Mn_6$ chain (feed back opened at $V_s$ = -2 V, $I_t$ = 1.5 nA). For comparison the conductance of the clean $Cu_2N$/Cu (100) surface is shown.

undistinguishable from the conductance background. On the contrary, the spectral intensity for the unoccupied state at the edges persists as the chain is reduced. The conductance map shows a localisation of the signal with increasing number of Mn atoms. Interestingly, the positive-energy state stays at the same energy position, independently of the chain's length, supporting its localised character.

### *4.2. Density functional theory characterisation of the electronic states*

Structural relaxation of the Mn atomic chains reproduce the geometry and bonding configuration from previous theoretical results [13, 16, 18]: Mn atoms induce an important reconstruction of the supporting substrate by incorporating N atoms to form

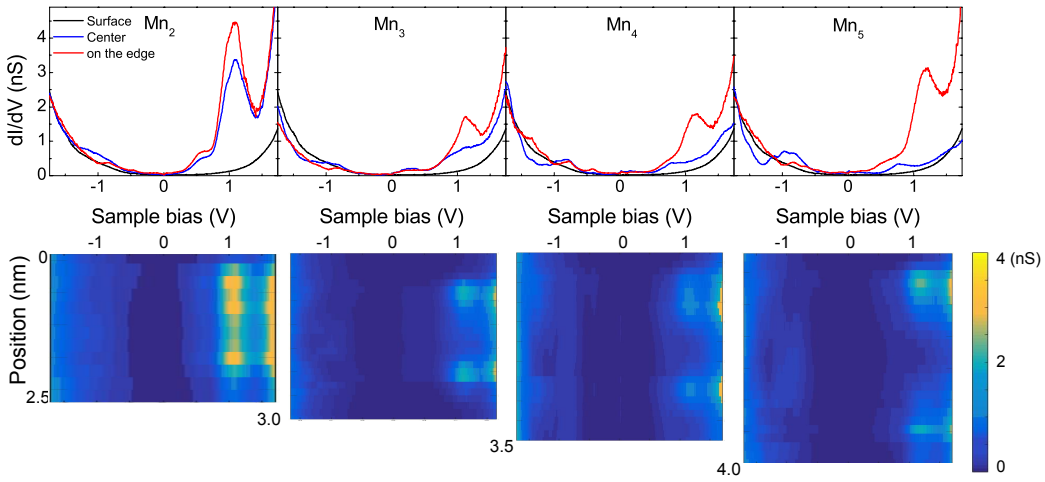


**Figure 2.** Tunnelling differential conductance measured over the edge (red), center(blue), and clean surface (black) for $Mn_2$, $Mn_3$, $Mn_4$, and $Mn_5$, upper row (feed back opened at $V_s$ = -2 V, $I_t$ = 1.5 nA). Plots of conductance (color scale) as a function of bias (x-axis) and position along the chain (y-axis), the plots extend slightly more than the chain sizes.

a Mn-N-Mn-N- $\cdots$ chain. This has important implications both for the electronic structure and the magnetic ordering of the atoms.

A consequence of the finite size of the chains is the apparition of additional localised states at the terminations due to the change of geometry. In strong correspondence with the experimental results, we find at $V_s$ $\sim$1 eV above the Fermi energy a state purely localised at the edges. This state, whose wave-function amplitude is depicted in Fig. 3($a$) for the case of a $Mn_3$ trimer has very little weight on atoms other than the two edge Mn atoms. It thus has a small intrinsic width.

The projected density of states (PDOS) gives us more information on the two states found in the STM studies (Figs. 1 and 2). The PDOS shows that these states are strictly spin polarised. The edge states only have contributions from $s$ and $d_{z^2}$ orbitals (where $z$ is the direction along the Mn chain). This leads to a sharp peak in the density of states projected onto the orbitals of the edge Mn atom, centred at $\sim$ 1 V, Fig. 3($b$). These data allow us to characterise the edge state as a Tamm state due to the unsaturated $s - dz^2$ hybrid orbital formed by the twisting of the chain at the edge.

The state at $\sim$ $-1$ eV is also found in DFT if the full electronic structure is projected onto the $p$ orbitals of the central N-atoms of the chain. Figure 3($b$) shows a sharp peak in the PDOS of the $p_z$ orbital of the third N atom in the $Mn_6$ chain. This allows us to characterise the experimental peak at $\sim -1$ V as a chain state originating in the N-atoms. The PDOS on the $p$ orbitals of the central N-atoms is identical for both spins, as we expected for electronic states with a strong N component. Hence, the experimental peak for occupied states corresponds to a state extended over the chain with a strong N character.

To explore the evolution the edge states with chain length we compare in Fig. 4 the

density of states projected on an edge Mn atom for $Mn_n$ chains with $n = 3, 4, 5, 6$. In agreement with the experimental results in Fig. 2, the edge state is observed pinned at $\sim 1$ eV and having basically the same shape regardless of the length of the chain. This is due to the large localisation of the state at the edge Mn atoms, thus interacting very weakly with the state at the other end.

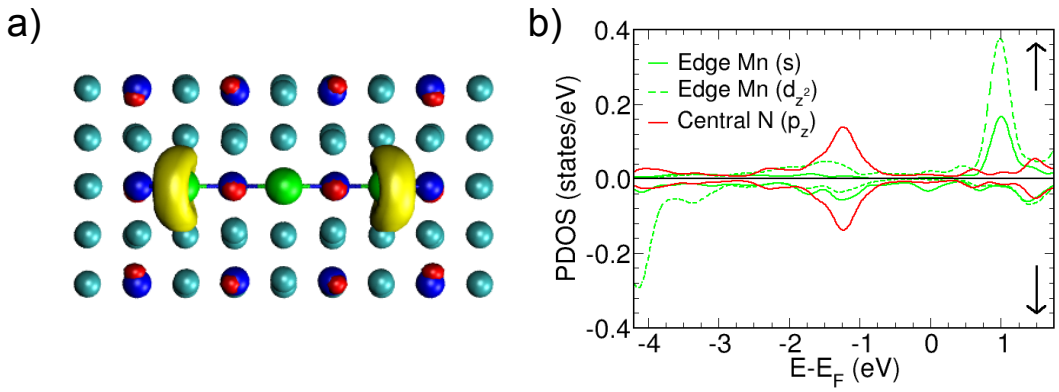


**Figure 3.** ($a$) Isosurface of wave-function amplitude of the edge state of an adsorbed $Mn_3$ chain. ($b$) PDOS of $Mn_6$ on the $p_z$ orbitals of N (where $z$ is the direction along the $Mn_6$ chain) and on the $s$ and $d_{z^2}$ electrons of a Mn edge atom.

In Fig. 4, we also observe that the edge state spin is anti-aligned with the spin of the edge atom (majority spin). However, previous studies [30, 31] showed that the electron transmission proceeded through the majority spin due to the prevailance of majority spin electrons at the Fermi energy. Figure 4 indeed shows that for Mn atomic chains the electron tunnelling transmission at low energies takes part mainly in the majority-spin channel, while at large positive energies the minority-spin components dominate the density of states.

## 5. Discussion

Figure 5($a$) shows isosurfaces of spin density for a $Mn_6$ atomic chain. In agreement with previous experimental studies [3], this corroborates that Mn atoms interact antiferromagnetically with their neighbours, as discussed by Rudenko *et al.* [13], and also by Nicklas *et al.* [16] for the case of Fe chains on the same substrate. The joining N atoms serve both to stabilise the chain via covalent bonding with the Mn atoms, and to induce the antiferromagnetic order through a superexchange interaction, clearly seen by the equal coexistence of the two spins on the N atoms in Fig. 5($a$). These results imply that the actual arrangement of Mn and N atoms does matter and different magnetic orderings can be achieved [18]. These results also show that the occupied electronic structure associated with N atoms must be spin unpolarised.

Figure 5($b$) plots the spin-polarised density of states projected onto Mn $d$-states. As previously mentioned [13, 14, 16, 18], the $d$ electrons maintain the free-atom configuration of Mn in the chains with all majority spin $d$-orbitals occupied and the

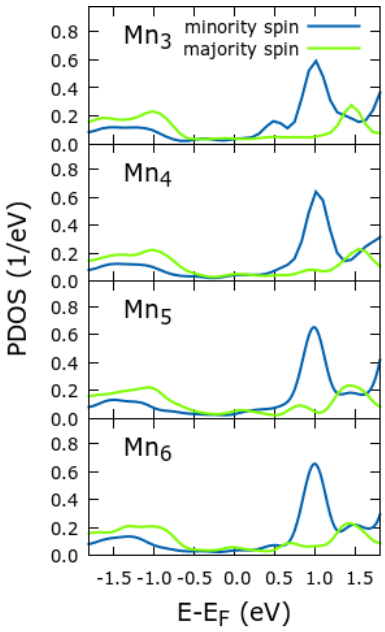


**Figure 4.** Projected density of states (PDOS) over all atomic orbitals of an edge Mn atom for $Mn_3$, $Mn_4$, $Mn_5$, and $Mn_6$ for majority and minority spins.

minority one empty. Figure 5($b$) also shows that the PDOS on $d$-electrons is mainly independent of the size of the Mn chains, indicating that their $d$-electron states are fairly localised and not perturbed by neighbouring Mn atoms.

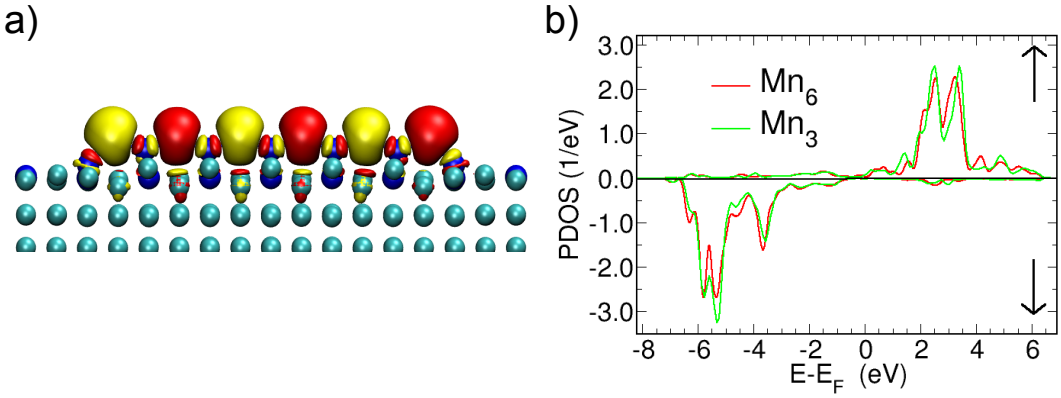


**Figure 5.** ($a$) Isosurface of spin density obtained as the difference of electronic density between the densities of majoritary (red) and minoritary (yellow) spins of a (broken-symmetry) DFT calculation. ($b$) Projected density of states (PDOS) over all Mn $d$-electrons of $Mn_6$ and $Mn_3$ showing minor differences, for the majority ($\downarrow$) and minority ($\uparrow$) spins.

The antiferromagnetic ordering of Mn chains on $Cu_2N$/Cu (100) was revealed by studying the spectra of low-energy excitations [3]. Even-numbered chains ($Mn_{2n}$ with $n$ integer) clearly show a step in the conductance that corresponds to a singlet-triplet excitation. The singlet ground state clearly shows the antiferromagnetic spin ordering

in the chain. Odd-numbered chains present steps in the conductance compatible with excitations in a system with a spin 5/2 ground state, again proving the antiferromagnetic structure of the chains. However, spin-polarised STM fails to detect the magnetic ordering of Mn chains. This is contrary to the case of antiferromagnetic Fe chains where Néel states are revealed by spin-polarised STM [5]. Indeed, the small magnetic anisotropy of Mn chains leads to very entangled spin structures different from the Fe chains [17, 32].

Experimentally, we find that the chains present localised states at the Mn edge atoms. Our DFT simulations show that the spin polarisation of the end states is connected to the spin of the terminal Mn atom. Therefore, the antiferromagnetic structure of the chains should dictate the relative spin of both ends, resulting in same or opposite spin for even or odd chains, respectively, for each of the antiferromagnetic configurations entering the magnetic ground state of the chain. Due to the antiferromagnetic spin structure of the chains we can expect to find an extraordinary localisation of the electronic states due to the spin structure for even-numbered chains.

## 6. Conclusions

In summary, we have investigated the electronic structure of Mn atomic chains constructed on $Cu_2N$/ Cu (100) by atomic manipulation. We have found two electronic states in the tunnelling spectra: an unoccupied Tamm state, very localised on the edge atoms and an occupied state extended along the chain. The unoccupied state presents a strict spin-polarisation, and is originated from the hybridization of Mn $d_{z^2}$ and $4s$ orbitals. The occupied state has weight on both N and Mn atoms and it is not spin polarised due to the absence of magnetism of the N atoms. We expect that in this model system, the parity of the number of atoms has an effect in their spectral fingerprint.

The existence of spin-polarised edge states may be quite ubiquitous on transition-metal magnetic chains, due to their general antiferromagnetic ordering and the weakening of bonds at the atomic edges. Their actual energy values may have important implications in their observation and on their impact on the electronic and magnetic properties of the chain.

## Acknowledgements

DJC acknowledges the European Union for support under the H2020-MSCA-IF-2014 Marie-Curie Individual Fellowship programme proposal number 654469. ICN2 acknowledges support from the Severo Ochoa Program (MINESCO, Grant SEV-2013-0295).

[1] H. Wang, Y. Yu, Y. Sun, and Q. Chen. Magnetic nanochains: a review. *NANO: Brief Reports and Reviews*, 6(1):1–17, 2011.

[2] Harald Brune. Assembly and probing of spin chains of finite size. *Science*, 312(5776):1005–1006, 2006.

[3] Cyrus F. Hirjibehedin, Christopher P. Lutz, and Andreas J. Heinrich. Spin coupling in engineered atomic structures. *Science*, 312(5776):1021–1024, 2006.

[4] A. A. Khajetoorians, J. Wiebe, B. Chilian, S. Lounis, S. Blügel, and R. Wiesendanger. Atom-by-atom engineering and magnetometry of tailored nanomagnets. *Nature Physics*, 8:497–503, 2012.

[5] Sebastian Loth, Susanne Baumann, Christopher P. Lutz, D. M. Eigler, and Andreas J. Heinrich. Bistability in atomic-scale antiferromagnets. *Science*, 335:196–199, 2012.

[6] Simon Holzberger, Tobias Schuh, Stefan Blügel, Samir Lounis, and Wulf Wulfhekel. Parity effect in the ground state localization of antiferromagnetic chains coupled to a ferromagnet. *Phys. Rev. Lett.*, 110:157206, Apr 2013.

[7] B. Bryant, A. Spinelli, J. J. T. Wagenaar, M. Gerrits, and A. F. Otte. Local control of single atom magnetocrystalline anisotropy. *Phys. Rev. Lett.*, 111:127203, Sep 2013.

[8] Shichao Yan, Deung-Jang Choi, Jacob A. J. Burgess, Steffen Rolf-Pissarczyk, and Sebastian Loth. Control of quantum magnets by atomic exchange bias. *Nature Nanotechnology*, 10:40–45, 2015.

[9] Roland Wiesendanger. Spin mapping at the nanoscale and atomic scale. *Rev. Mod. Phys.*, 81:1495–1550, Nov 2009.

[10] A. J. Heinrich, J. A. Gupta, C. P. Lutz, and D. M. Eigler. Single-atom spin-flip spectroscopy. *Science*, 306(5695):466–469, 2004.

[11] Jean-Pierre Gauyacq, Nicolás Lorente, and Frederico Dutilh Novaes. Excitation of local magnetic moments by tunneling electrons. *Progress in Surface Science*, 87(5-8):63–107, 2012.

[12] Samir Lounis, Peter H. Dederichs, and Stefan Blügel. Magnetism of nanowires driven by novel even-odd effects. *Phys. Rev. Lett.*, 101:107204, Sep 2008.

[13] A. N. Rudenko, V. V. Mazurenko, V. I. Anisimov, and A. I. Lichtenstein. Weak ferromagnetism in mn nanochains on the CuN surface. *Physical Review B*, 79(14):144418, 2009.

[14] Chiung-Yuan Lin and B. A. Jones. First-principles calculations of engineered surface spin structures. *Phys. Rev. B*, 83:014413, Jan 2011.

[15] Cyrus F. Hirjibehedin, Chiung-Yuan Lin, Alexander F. Otte, Markus Ternes, Christopher P. Lutz, Barbara A. Jones, and Andreas J. Heinrich. Large magnetic anisotropy of a single atomic spin embedded in a surface molecular network. *Science*, 317(5842):1199–1203, 2007.

[16] Jeremy W. Nicklas, Amita Wadehra, and John W. Wilkins. Magnetic properties of fe chains on $Cu_2N$/Cu(100): A density functional theory study. *Journal of Applied Physics*, 110(12):123915, 2011.

[17] Jean-Pierre Gauyacq, Simeón Moisés Yaro, Xavier Cartoixà, and Nicolás Lorente. Correlation-mediated processes for electron-induced switching between nel states of fe antiferromagnetic chains. *Phys. Rev. Lett.*, 110:087201, Feb 2013.

[18] M. C. Urdaniz, M. A. Barral, and A. M. Llois. Magnetic exchange coupling in $3d$-transition-metal atomic chains adsorbed on $Cu_2N$/Cu(001). *Phys. Rev. B*, 86:245416, Dec 2012.

[19] Benjamin Bryant, Ranko Toskovic, Alejandro Ferron, Jose L. Lado, Anna Spinelli, Joaquin Fernandez-Rossier, and Alexander F. Otte. Controlled complete suppression of single-atom inelastic spin and orbital cotunneling. *Nano Letters*, 15(10):6542–6546, 2015.

[20] Kun Tao, Qing Guo, Puru Jena, Desheng Xue, and Valeri S. Stepanyuk. Tuning magnetic properties of antiferromagnetic chains by exchange interactions: ab initio studies. *Phys. Chem. Chem. Phys.*, 17:26302–26306, 2015.

[21] A Spinelli, M P Rebergen, and A F Otte. Atomically crafted spin lattices as model systems for quantum magnetism. *Journal of Physics: Condensed Matter*, 27(24):243203, 2015.

[22] M. C. Desjonquères and D. Spanjaard. *Concepts in Surface Physics*. Springer-Verlag, 1996.

[23] F. M. Leibsle, C. F. J. Flipse, and A. W. Robinson. Structure of the cu100- $cu_2n$ surface: A scanning-tunneling-microscopy study. *Phys. Rev. B*, 47:15865–15868, Jun 1993.

[24] T. Choi, C. D. Ruggiero, and J. A. Gupta. Tunneling spectroscopy of ultrathin insulating cu2n films, and single co adatoms. *Journal of Vacuum Science & Technology B*, 27(2):887–890, 2009.

[25] G. Kresse and J. Furthmüller. Efficiency of ab-initio total energy calculations for metals and

semiconductors using a plane-wave basis set. *Computational Materials Science*, 6(1):15–50, 1996.

[26] P. E. Blöchl. Projector augmented-wave method. *Physical Review B*, 50(24):17953, 1994.

[27] G. Kresse and D. Joubert. From ultrasoft pseudopotentials to the projector augmented-wave method. *Physical Review B*, 59(3):1758, 1999.

[28] John P. Perdew, Kieron Burke, and Matthias Ernzerhof. Generalized gradient approximation made simple. *Physical Review Letters*, 77(18):3865, 1996.

[29] S. L. Dudarev, G. A. Botton, S. Y. Savrasov, C. J. Humphreys, and A. P. Sutton. Electron-energy-loss spectra and the structural stability of nickel oxide:an LSDA+U study. *Physical Review B*, 57(3):1505, 1998.

[30] Nicolás Lorente and Jean-Pierre Gauyacq. Efficient spin transitions in inelastic electron tunneling spectroscopy. *Phys. Rev. Lett.*, 103:176601, Oct 2009.

[31] Frederico D. Novaes, Nicolás Lorente, and Jean-Pierre Gauyacq. Quenching of magnetic excitations in single adsorbates at surfaces: Mn on CuN/Cu(100). *Phys. Rev. B*, 82:155401, Oct 2010.

[32] Jean-Pierre Gauyacq and Nicolás Lorente. Decoherence-governed magnetic-moment dynamics of supported atomic objects. *Journal of Physics: Condensed Matter*, 27(45):455301, 2015.